Decreasing waste brine in anion exchange with nanofiltration: Implications for multiple treatment cycles

Supplemental Information

Julie A. Korak[1], Leah Flint[1,2], Miguel Arias-Paic[2]

[1]Department of Civil, Environmental, and Architectural Engineering, University of Colorado Boulder, UCB 607, Boulder, CO 80303

[2]Bureau of Reclamation, Department of the Interior, PO Box 25007, Denver, CO 80225

Table of Contents

1 Safety and Hazards

1.1 Nanofiltration experiments

The bench-scale nanofiltration experiments used synthetic solutions containing sodium chloride, sodium sulfate, sodium nitrate, and sodium bicarbonate, which were pH was adjusted with sodium hydroxide. Appropriate personal protective equipment (PPE) and safe handling are necessary for all chemical risks.

The bench-scale membrane system operated at high pressure (150-250 psi). The system was leak tested at low pressure prior to conducting high pressure experiments. System materials and fittings were rated for the high pressure application. Eye protection was worn at all times in case of high pressure process failure. Situational awareness for electrical risks (i.e., 220 V power supply) and physical risks (i.e., slip and trip hazards) was also practiced.

1.2 Ion exchange experiments

There were several chemical safety hazards during regeneration experiments. Trace metals accumulated during the water treatment loading process and eluted as a highly concentrated solution during regeneration. These experiments produced hazardous concentrations of hexavalent chromium, arsenic, vanadium, uranium, and selenium. Batch regeneration also used concentrated solutions of hydrochloric acid, which is corrosive and a chemical hazard. PPE, careful sample handling, and workplace hygiene were necessary to mitigate risks. Regeneration samples were handled and disposed as hazardous waste.

2 Field site

Table S1 presents the raw water quality for the groundwater well in Oklahoma used to load the pilot-scale columns. Figure S1 shows the process flow diagram used to load columns in parallel. Breakthrough curves for the first loading cycle are presented in Figure S2. A total of 5 columns were loaded, but only three were used in this study. The bed volume for each column was 1.2 L. The raw water was filtered through spun depth cartridge filters with a minimum pore size of 5 μm to remove coarse sediment. Table S2 summarizes the assumed anionic form for oxyanions under oxidizing conditions and the groundwater pH of 8.3.

Table S1. Groundwater quality for test site in Norman, OK

	Parameter	Units	Average ± Standard Deviation (n=3)
Bulk Water	pH	SU	8.3 ± 0.1
	Total Alkalinity	mg/L as $CaCO_3$	276 ± 23
	DO	mg/L	6.2 ± 0.7
	TDS	mg/L	381 ± 4
	Conductivity	μS/cm	538 ± 8
	Dissolved Organic Carbon	mg/L	1.0 ± 0.12
Cations	Calcium	mg/L	8.4 ± 0.5
	Potassium	mg/L	1.9 ± 0.12
	Magnesium	mg/L	4.9 ± 0.3
	Sodium	mg/L	105 ± 7.7
Anions	Chloride	mg/L	17.0 ± 0.5
	Sulfate	mg/L	13.8 ± 1.4
	Perchlorate	μg/L	<4.00
	Nitrate-Nitrate Nitrogen	mg/L	0.36 ± 0.03
Metals	Iron, Total	mg/L	<0.025
	Arsenic, Total	μg/L	6.4 ± 0.8
	Chromium, Total	μg/L	85.8 ± 0.4
	Chromium, Hexavalent	μg/L	87.8 ± 1.0
	Molybdenum, Total	μg/L	3.9 ± 0.04
	Manganese, Total	mg/L	<0.001
	Vanadium, Total	μg/L	103 ± 4
	Uranium, Total	mg/L	14 ± 0.3

Table S2. Assumed anionic form for oxyanions under oxidizing conditions and groundwater pH

Analyte	Assumed Anionic Form	Reference
Cr	CrO_4^{2-}	(SenGupta and Clifford, 1986)
V	$H_2VO_4^-$	(Wright et al., 2014)
U	$UO_2(CO_3)_3^{4-}$	(Langmuir, 1978; Zhang and Clifford, 1994)
Se	SeO_4^{2-}	(White and Dubrovsky, 1994)
As	$HAsO_4^{2-}$	(Bissen and Frimmel, 2003)
Mo	MoO_4^{2-}	(SenGupta, 1986)

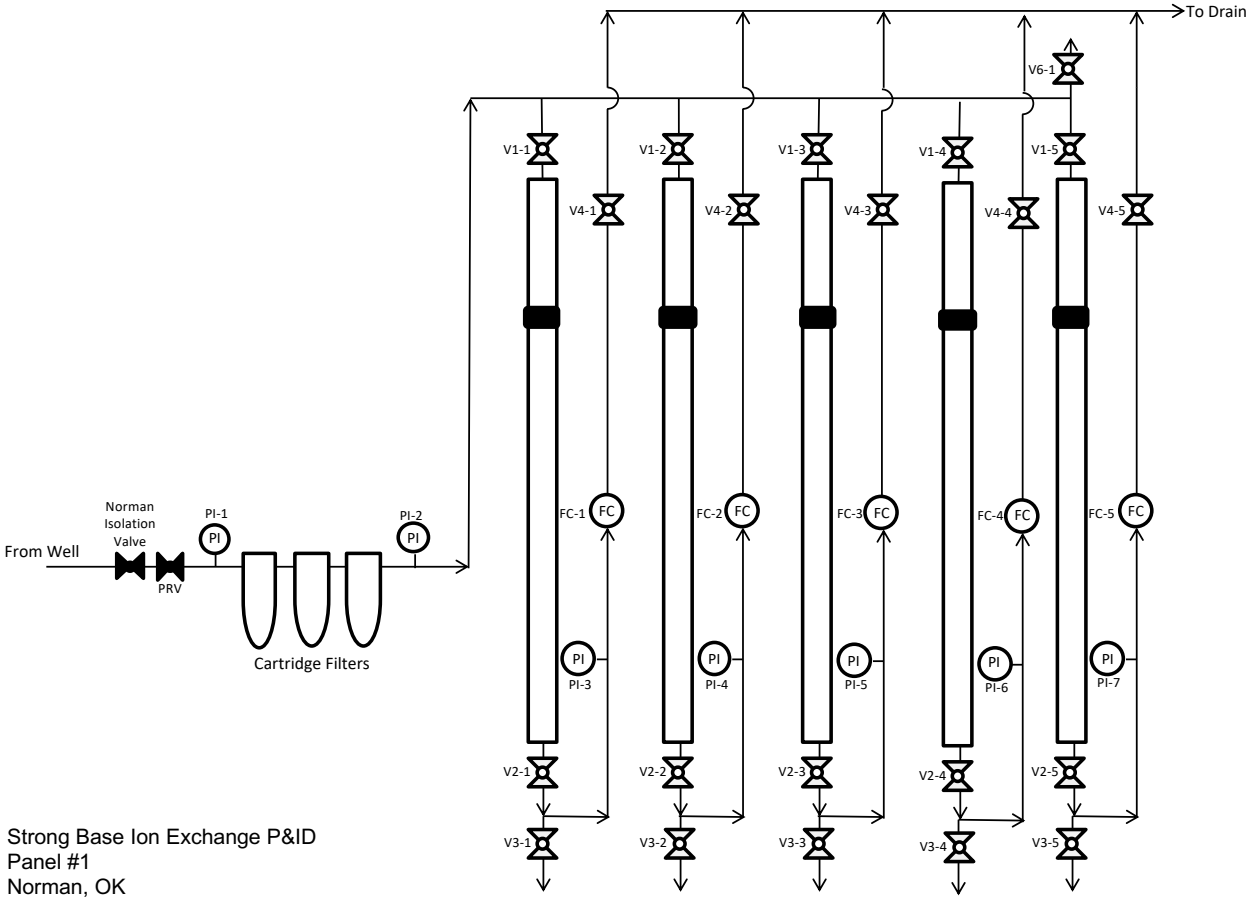

Figure S1. Process flow diagram for column loading. Only three of the five columns were used in this study.

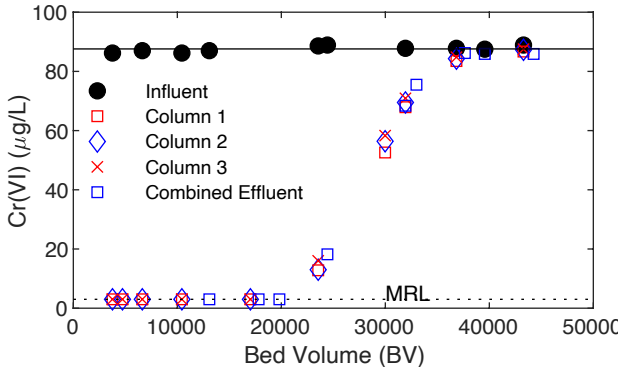

Figure S2. Pilot-scale loading of 3 columns reported in this study and the combined effluent from 5 parallel columns loaded simultaneously (2 columns not used in this study). The method reporting limit (MRL) was 3 µg/L.

3 Supplemental Regeneration Results

The comparison of the cumulative elution of each constituent for the 1- and 2-Stage regeneration approaches using fresh regeneration solutions is shown in Figure S3. The cumulative recovery of sulfate, nitrate, inorganic carbon, uranium and vanadium were comparable between both approaches. Vanadium was steadily eluting at the end of the 2 N regeneration stage and similar total recoveries were observed, because the same volume of 2 N NaCl solution was used.

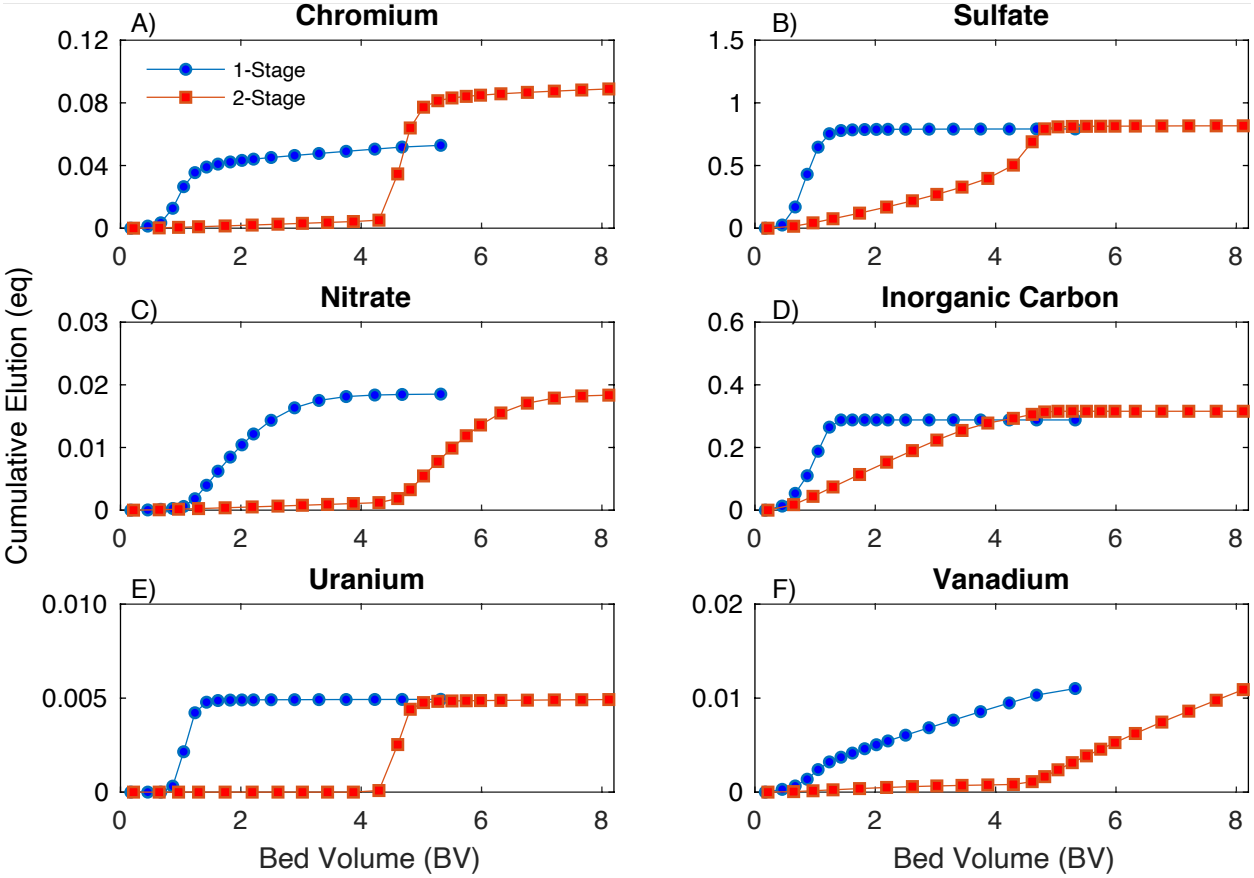

Figure S3. Cumulative elution during 1- and 2-Stage regenerations using fresh regeneration solution

4 Cyclical Brine Reuse Model

This section documents the calculations for the cyclical process model incorporating the assumptions and constraints outlined in Section 3 of the main text.

1. **The criteria for diverting waste brine to the Flex 1 and Collection Vessels is** based on experimental data. The starting bed volume (BV_{start}) is determined by the conductivity setpoint (20 mS/cm) specified by model constraint 3 (Section 3 of main text). The ending bed volume (BV_{end}) is determined by 99% nitrate elution (model constraint 4). The waste collected in the Collection Vessel for each regeneration approach is outlined in Table S3 for the pilot-scale data from the Oklahoma test site (Figure 2 in main text).

Table S3. Waste fractionation for the NF- reuse model for 1- and 2-Stage regeneration approaches

Vessel	Start	Stop	Model	
			1-Stage	2-Stage
Flex 1	BV=0	BV_{start} (1)	0 to 0.3 BV	0 to 4.0 BV
Collection	BV_{start} (1)	BV_{end} (2)	0.3 to 4.5 BV	4.0 to 8 BV
Notes (1) BV_{start} is defined by the conductivity setpoint (i.e., $Cond_{sp}$=20 mS/cm) (2) BV_{end} is determined based on equivalent and complete nitrate elution.				

2. **Initial conditions for fresh regeneration solution are shown in Table S4.**

Table S4. Initial conditions for the NF-reuse model

Variable	Initial
Regeneration solution volume	V_R *defined from experimental data using Equation 6 in main text.*
Initial sodium concentration	$[Na]_{R,0} = 2\frac{eq}{L}$
Initial chloride concentration	$[Cl]_{R,0} = 2\frac{eq}{L}$
Initial concentration of exchangeable anions	$[An]_{R,0} = 0\frac{eq}{L}$ where An is defined individually for SO_4^{2-}, NO_3^-, HCO_3^-, or the anionic forms of Cr, V, Se, As, Mo, and U

Model constraint 1 (Section 3 of main text) assumes that the regeneration solution volume (V_R) is constant across multiple process cycles. BV_{end} is set based on nitrate elution (constraint 4), and Table S3 determines the volume of initial regeneration solution (V_R) needed to reach BV_{end} from experimental data. Assuming sodium is a conservative tracer and its concentration in the interstitial water is negligible, a mass balance formula (Equation S 1) integrates the experimental data and calculates the total amount of sodium that passes through the Contactor between BV_{start} and BV_{end}. The volume of interstitial water (V_{IS}) captured in the Disposal Vessel is calculated using Equation S 2.

$$[Na]_{R,0}V_R = \int_{BV_{start}\cdot V_{resin}}^{BV_{end}\cdot V_{resin}} [Na]dV$$

Equation S 1

$$V_{IS} = V_{resin}(BV_{end} - BV_{start}) - V_R$$ **Equation S 2**

where $[Na]_{R,0} = 2\ eq/L$

V_{resin} is the volume of resin in the contactor

3. **The volume ($V_{w,i,0}$) and composition of waste brine diverted to the Collection Vessel** can be determined by Equation S 3 and Equation S 4. $\mathbf{V_{w,i,0}}$ includes waste brine from BV_{start} to BV_{end}, interstitial water (V_{IS}), and a set amount of rinse water, and *i* indicates the reuse cycle (*i*=0 for fresh brine).

$$V_{w,i,0} = (BV_{end} - BV_{start})V_{resin} + V_{rinse}$$ **Equation S 3**

$$V_{rinse} = 0.5\ V_{resin}$$ **Equation S 4**

Composition is calculated from the pilot data assuming that the same mass and composition of anions accumulates on and releases from the resin during each cycle. This is a conservative assumption, because it assumes that the loading and regeneration efficiency is unaffected by impurities in the regeneration solution or incomplete regeneration. The validity of this assumption is a primary objective of this study and is tested using a synthetic solution based on the cyclical process model results (Section 4.4 in main text).

The total mass of each anion (An) that is captured in the Collection Vessel (ΔM_{An}) is calculated by integrating the pilot-scale regeneration data between BV_{start} and BV_{end} (Equation S 5). The mass of chloride that exchanges onto the resin (ΔM_{Cl}) is calculated as the sum of all anions that exchanged off the resin (Equation S 6).

$$\Delta M_{An} = \int_{BV_{reuse} \cdot V_{resin}}^{BV_{end} \cdot V_{resin}} [An]\ dV$$ **Equation S 5**

$$\Delta M_{Cl} = \sum_{all\ An} \Delta M_{An}$$ **Equation S 6**

where

[An] is the concentration of any anion other than chloride in units of eq/L. “An” is defined individually for SO_4^{2-}, NO_3^-, HCO_3^-, and the assumed oxyanion forms of Cr, V, Se, As, Mo, and U.

ΔM_{An} is the mass of any anion other than chloride in units of eq

The concentration of each exchangeable anion (An), except chloride, is calculated by a mass balance using Equation S 7. This calculation considers that only a portion of the

waste collected ($V_{w,I,0}$-V_{IS}-V_{rinse}) had a background concentration of impurity anions in the regeneration solution ($[An]_{R,i}$) by subtracting the interstitial water volume (V_{IS}) (Equation S 2) and rinse water volume (V_{rinse}) (Equation S 4).

$$[An]_{w,i,0} = \frac{[An]_{R,i} \cdot (V_{w,i,0} - V_{rinse} - V_{IS}) + \Delta M_{An}}{V_{w,i,0}} \quad \textbf{Equation S 7}$$

The concentration of chloride in the Collection Vessel is determined using a mass balance (Equation S 8), accounting for the interstitial and rinse water volumes, by assuming the amount of chloride that exchanges onto the resin equals the sum of all anions eluted from the resin.

$$[Cl]_{D,i} = \frac{[Cl]_R \cdot (V_{w,i,0} - V_{rinse} - V_{IS}) - \Delta M_{Cl}}{V_{D,i}} \quad \textbf{Equation S 8}$$

4. **The iterative nanofiltration process model is implemented to determine volume and composition of brine in the Collection** ($V_{w,i,RecMax}$, $[Cl]_{w,i,RecMax}$, $[Na]_{w,i,RecMax}$, $[An]_{w,i,RecMax}$) **and Permeate Vessels** ($V_{Pcomp,RecMax}$, $[Cl]_{Pcomp,i,RecMax}$, $[Na]_{Pcomp,i,RecMax}$, $[An]_{Pcomp,i,RecMax}$) at the maximum recovery (RecMax). **See SI Section 5.3 for details of the nanofiltration batch model.**

5. **A chloride (Equation S 9) and water balance (Equation S 10), determines the water and salt make-up needed for the next regeneration (Equation S 11 and Equation S 12).** The model assumes that the start of each regeneration process is constrained by constant values for $[Cl]_R$ and V_R that do not change as a function of regeneration cycle (*i*). Using the composite chloride concentration in the Permeate Vessel, the volumes of permeate and saturated salt required for the next regeneration are calculated, *assuming nanofiltration can produce sufficient permeate prior to flux limitations*.

$$[Cl]_R \cdot V_R = [Cl]_{Pcomp,i,RecMax} \cdot V_{RU,i} + [Cl]_{sat} \cdot V_{sat,i} \quad \textbf{Equation S 9}$$

$$V_R = V_{RU,i} + V_{sat,i} \quad \textbf{Equation S 10}$$

$$V_{sat,i} = \frac{V_R \cdot ([Cl]_R - [Cl]_{Pcomp,i,RecMax})}{([Cl]_{sat} - [Cl]_{Pcomp,i,RecMax})} \quad \textbf{Equation S 11}$$

$$V_{RU,i} = V_{R,i} - V_{sat,i} \quad \textbf{Equation S 12}$$

The volume of recycled brine needed ($V_{RU,i}$) is compared to the volume of permeate produced ($V_{P,i,RecMax}$), then the decision tree with Equation S 13 to Equation S 18 is used to determine the actual volumes of makeup water ($V_{H2O,i}$) and excess permeate ($V_{EP,i}$).

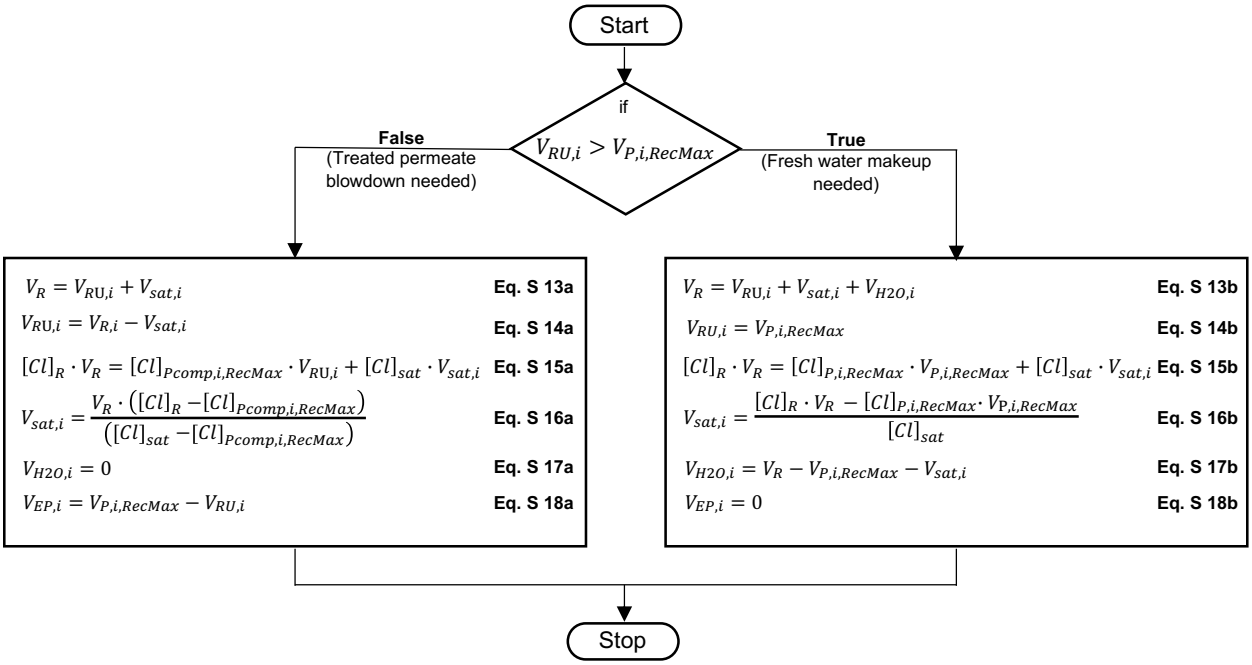

Figure S4. Decision tree to determine mass balance equations depending on nanofiltration permeate production

6. **The composition of the NF-reuse brine after make-up salt and water addition is determined (if needed) for the next regeneration (*i*+1) after dilution.**

$$[An]_{R,i+1} = \frac{[An]_{Pcomp,i,RecMax} \cdot V_{RU,i}}{V_R} \quad \textbf{Equation S 19}$$

$$[Na]_{R,i+1} = [Cl]_R + \sum [An]_{R,i} \quad \textbf{Equation S 20}$$

7. **Calculate the volume and composition of waste in the Disposal Vessel.** After waste concentration by NF, remaining concentrate is sent as blowdown (V_{BD}) to the Disposal Vessel where it is combined with concentrated NF waste from previous regeneration cycle (i-1).

$$V_{BD,i} = V_{w,i,RecMax} \quad \textbf{Equation S 21}$$

$$V_{D,i} = V_{D,i-1} + V_{BD,i} \quad \textbf{Equation S 22}$$

$$[An]_{D,i} = \frac{[An]_{w,i,RecMax} V_{BD,i} + [An]_{D,i-1} V_{D,i-1}}{V_{D,i}} \quad \textbf{Equation S 23}$$

$$[Cl]_{D,i} = \frac{[Cl]_{w,i,RecMax} V_{BD,i} + [Cl]_{D,i-1} V_{D,i-1}}{V_{D,i}} \quad \textbf{Equation S 24}$$

$$[Na]_{D,i} = \frac{[Na]_{w,i,RecMax} V_{BD,i} + [Na]_{D,i-1} V_{D,i-1}}{V_{D,i}} \quad \textbf{Equation S 25}$$

8. The regeneration cycle is complete. Repeat steps 3-7 for the next cycle (*i*+1).

5 Batch Nanofiltration Model

This section outlines the assumptions and response surfaces implemented into a batch nanofiltration model. The goal is not to develop a mechanistic model, but a practical one that can predict how impurities might accumulate in NF-reuse brine to inform future experiments.

5.1 Experimental Approach

Korak et al. (2018) developed empirical relationships for flux and chloride rejection using pilot-scale waste brine, but this approach was limited by confounding experimental variables. Chloride and sulfate concentration could not be varied independently using field SBIX brines (Korak et al., 2018). To make the empirical relationships more robust, synthetic solutions containing a range of chloride and sulfate concentrations were evaluated to test the importance of composition and TMP on both flux and rejection. The synthetic solutions also contained a representative concentration of nitrate for this source water to develop a predictive relationship for nitrate rejection as a function of composition and TMP. The experimental matrix is summarized in Table S5.

Table S5 summarizes the compositions of the synthetic solutions depicted in Figure 1 in the main text. The nitrate concentration was representative of the composite waste brine from the Oklahoma field site after a 1-Stage regeneration using 4 BV of 2 N NaCl. Experiments were conducted in 4 batches, starting with an initial solution containing sodium chloride, sodium nitrate and sodium bicarbonate for buffering capacity. Sodium sulfate was added sequentially, starting with the second test condition, to increase the concentration. The feed solution pH was adjusted to 8.5 as needed using sodium hydroxide (NaOH).

Table S5. Composition of synthetic solutions representative of SBIX brines for nanofiltration tests

Batch	Feed Solution Composition						
	$[Cl^-]$ (eq/L)	$[NO_3^-]$ (meq/L)	$[SO_4^{2-}]$ (eq/L)				
1	1.15±0.01	3.0±0.3	0	0.40±0.01	0.84±0.003	1.26	N/A
2	1.33±0.02	2.7±0.2	0	0.37±0.003	0.76±0.002	1.18	1.36
3	1.49±0.02	2.5±0.2	0	0.36±0.002	0.74±0.004	1.11	1.30
4	1.70±0.04	2.7±0.2	0	0.36±0.003	0.79±0.03	1.11	1.29

Feed solution pH adjusted to 8.5 with NaOH and buffered with 1.67 meq/L $NaHCO_3$.

For each batch, chloride and nitrate concentrations were nominally constant and sulfate was added sequentially to test concentrations ranging from 0 to 1.36 eq/L.

Uncertainty represents the standard deviation of feed samples collected in triplicate.

Figure S5 illustrates the process flow diagram for the bench-scale nanofiltration unit. For the synthetic SBIX solutions, the unit was operated under full-recycle. Following a 15-minute stabilization period, permeate was diverted to a balance for flux measurements and sample collection.

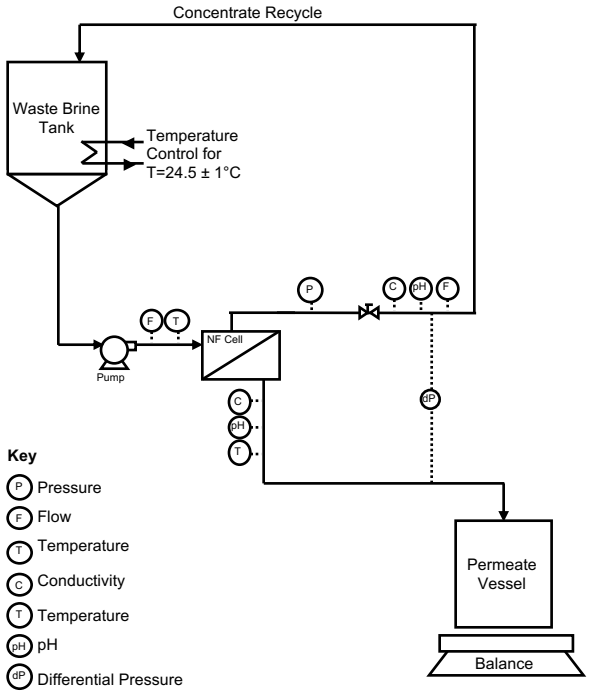

Figure S5. Process flow diagram for bench-scale nanofiltration unit.

5.2 Nanofiltration response surface models

5.2.1 Empirical flux relationships at 250 psi

Using Korak et al. (2018) as a starting place, the exponential relationship relating flux and sulfate concentration was fit using synthetic solutions from this study. Although the model parameters agreed well with the prior referenced study (Figure S6a), Figure S6b shows that the empirical model does not have constant variance, which is a requirement for robust regression models. A variance stabilizing transformation of the response data (i.e., flux) was applied by taking the natural logarithm of the flux, and a new stepwise model fit. A residuals analysis shows systemic behavior with respect to chloride concentrations in Figure S7c, demonstrating that chloride concentration is an important factor that was not captured in the 2018 study.

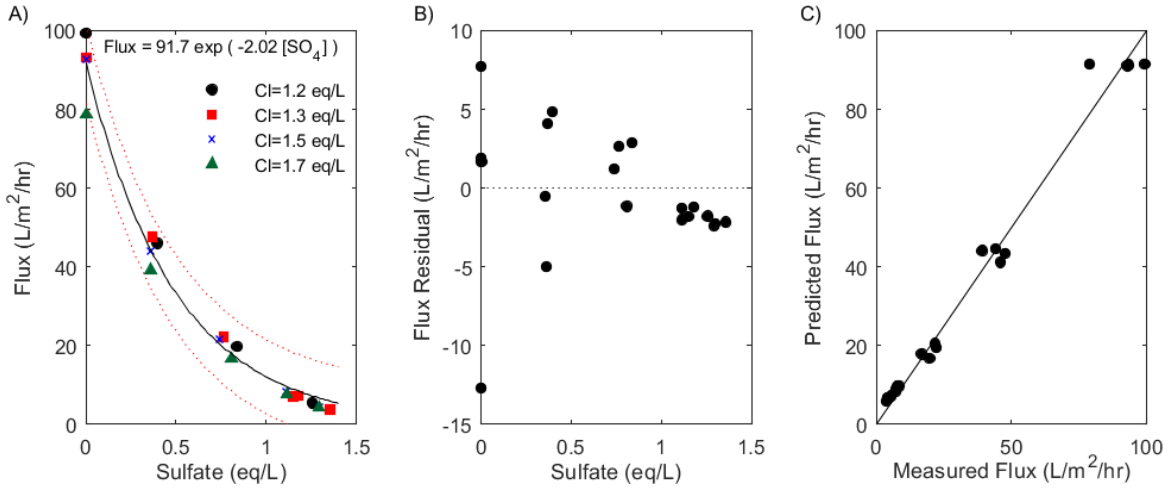

Figure S6. Empirical relationship between sulfate concentration and flux for synthetic brine solutions using an exponential function at 250 psi TMP

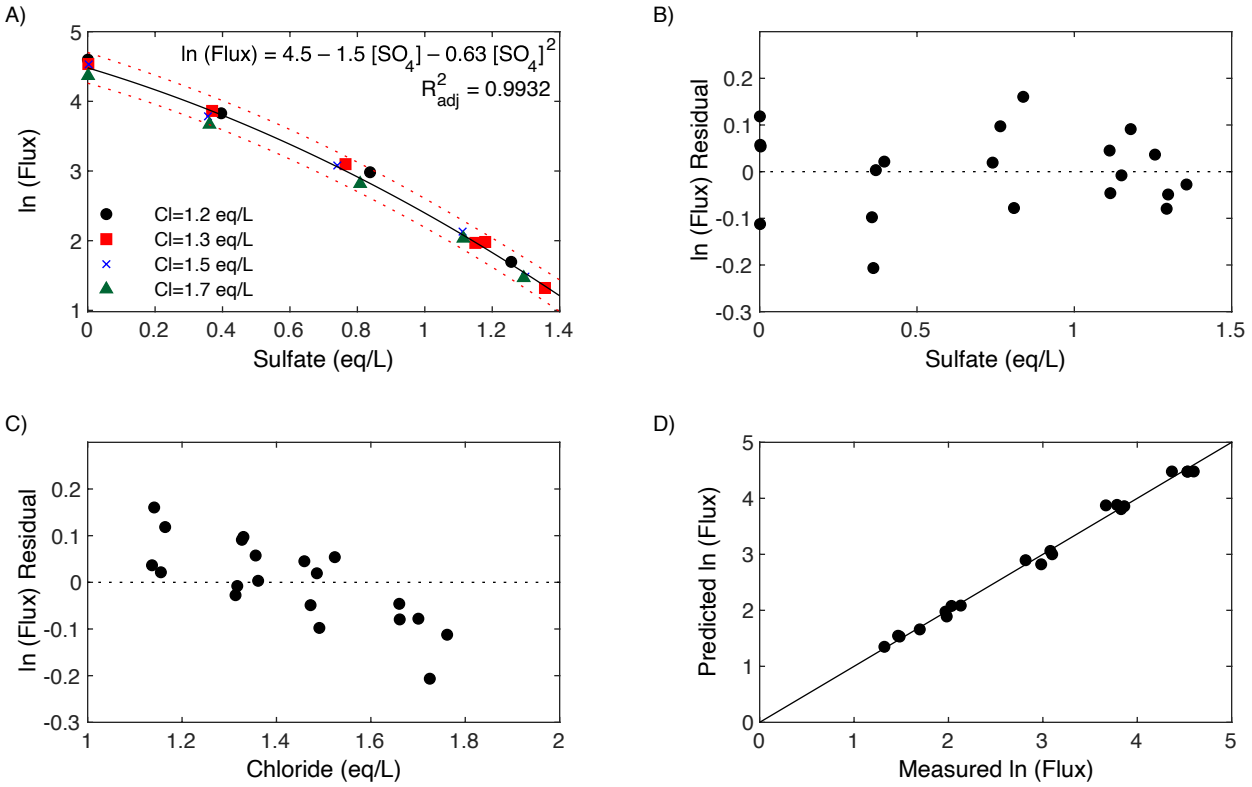

Figure S7. Empirical relationship between sulfate concentration and the natural log of flux for synthetic brine solutions at 250 psi TMP

Using the transformed response variable (ln(Flux)), a multilinear response surface using sulfate and chloride concentrations as independent variables was developed. Regressions up to a second order model, which includes quadratic and interaction terms, were evaluated using a forward and backward stepwise approach. Figure S8a shows the response surface for the best fit regression includes first and second order terms for sulfate and a first order term for chloride. The R^2_{adj} for this model was slightly higher than the model in Figure S7. The residuals are random with respect to chloride, exhibit some clustering at low sulfate concentration, and agree with a normal distribution assumption (Anderson Darling $p>0.05$). Figure S9 shows the response surface with the response variable units transformed back to flux in $L/m^2/hr$.

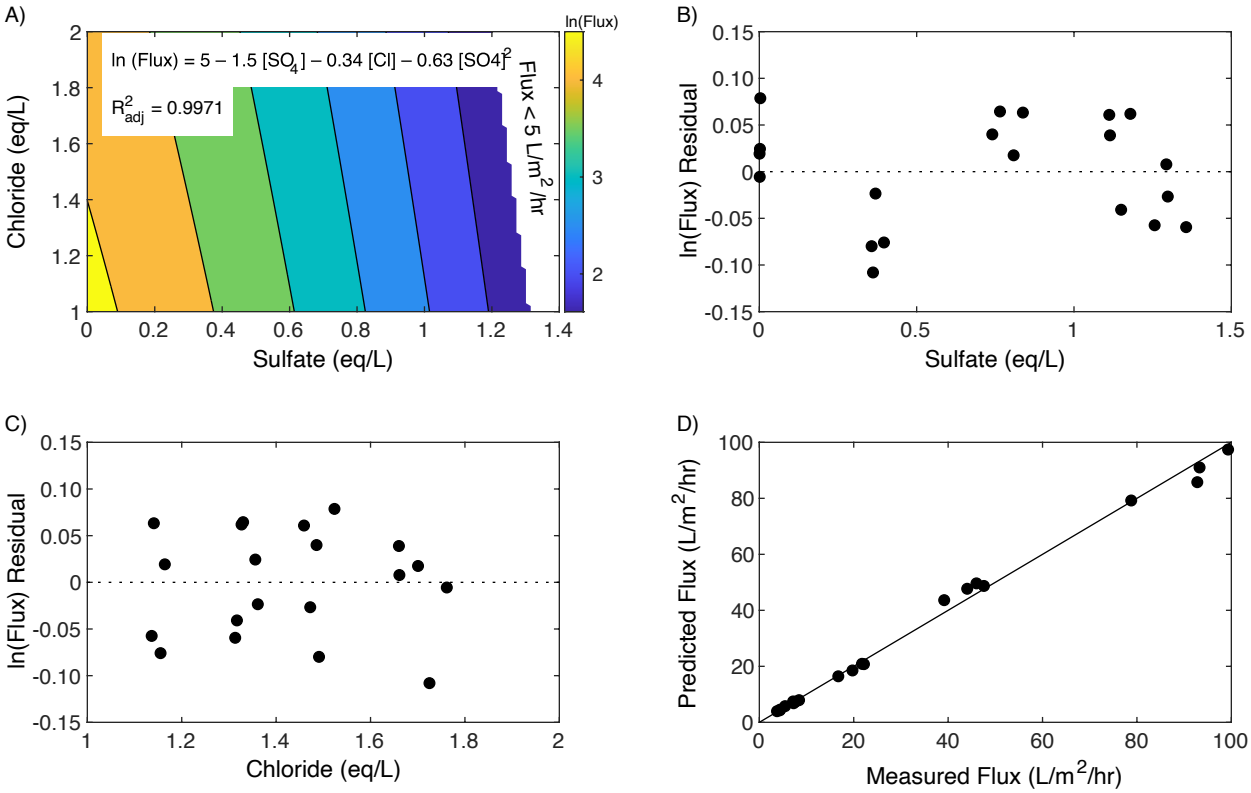

Figure S8. Response surface model predicting ln(Flux) as a function of both sulfate and chloride concentration at 250 psi TMP

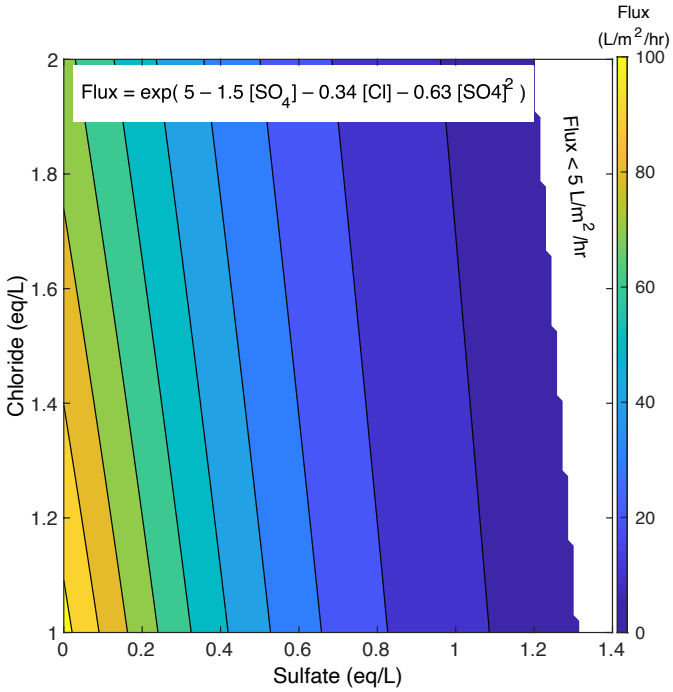

Figure S9. Response surface model predicting ln(Flux) as a function of both sulfate and chloride concentration at 250 psi TMP.

5.2.2 Response surfaces for membrane rejection at 250 psi

A similar approach was used to develop response surfaces that predict rejection as a function of the waste composition assuming operation at a constant TMP of 250 psi. Response surface models were fit using a stepwise multilinear regression, where terms are added sequentially based on p values. Model adequacy was assessed according to parameter significance and residual analysis. Figure S10 presents a response surface model for chloride rejection, which includes both main effects for sulfate and chloride concentration, an interaction term, and a second order term for sulfate concentration. All terms were statistically significant with coefficient p values less than 0.01. Term significance was confirmed using standardized independent variables.

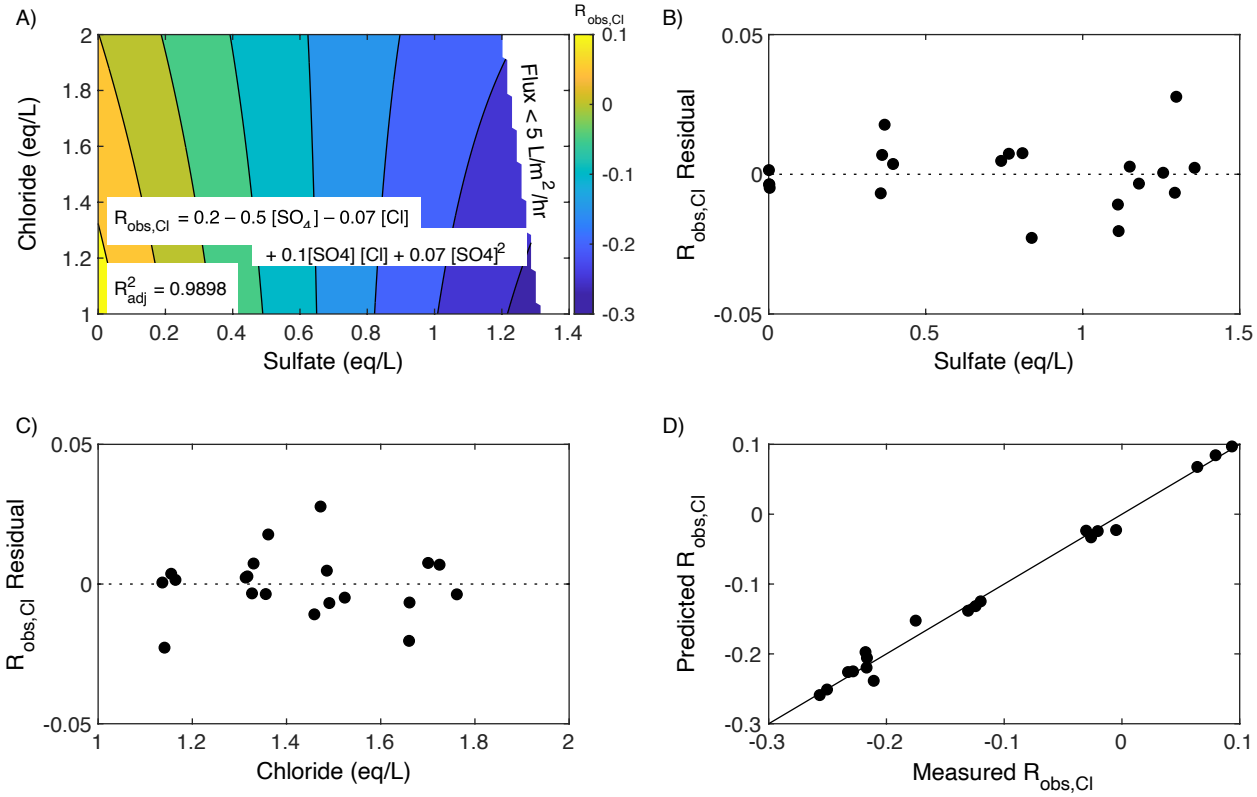

Figure S10. Response surface predicting chloride rejection as a function of both sulfate concentration at 250 psi TMP

Figure S11 presents a response surface model for nitrate rejection. In general, model fits for nitrate rejection, as assessed by R^2_{adj}, were lower than flux and chloride rejection models. Nitrate concentrations were several orders of magnitude lower than chloride and sulfate, which led to more analytical uncertainty. Sulfate concentrations alone could not adequately model nitrate rejection indicated by systematic residuals. A response surface with chloride and sulfate as independent variables had random, normally-distributed residuals with an R^2_{adj} of 0.898. Model residuals were less than 0.05 across experimental conditions.

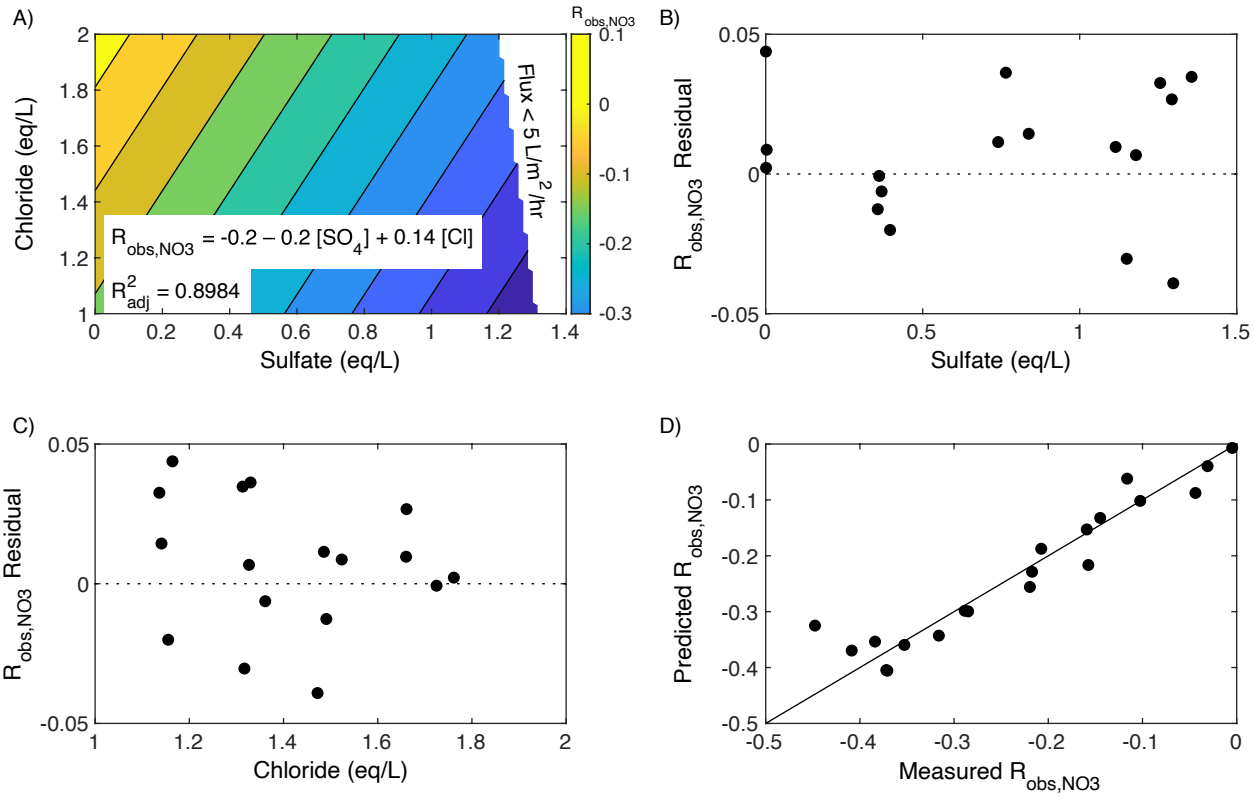

Figure S11. Response surface predicting nitrate rejection as a function of sulfate and chloride concentrations at 250 psi TMP

Lastly, a response surface for sulfate rejection was developed. A preliminary screening found that sulfate rejection depended on sulfate concentration and flux but not chloride concentration. A second order response surface using sulfate concentration fit the collected data at concentrations above 0.5 eq/L sulfate, but it did not give adequate predictions at lower sulfate concentrations. Therefore, a nonlinear logarithmic relationship using ln(Flux) as an independent variable was fit to the experimental data to provide realistic projections for the range of sulfate concentrations evaluated as shown in Figure S12.

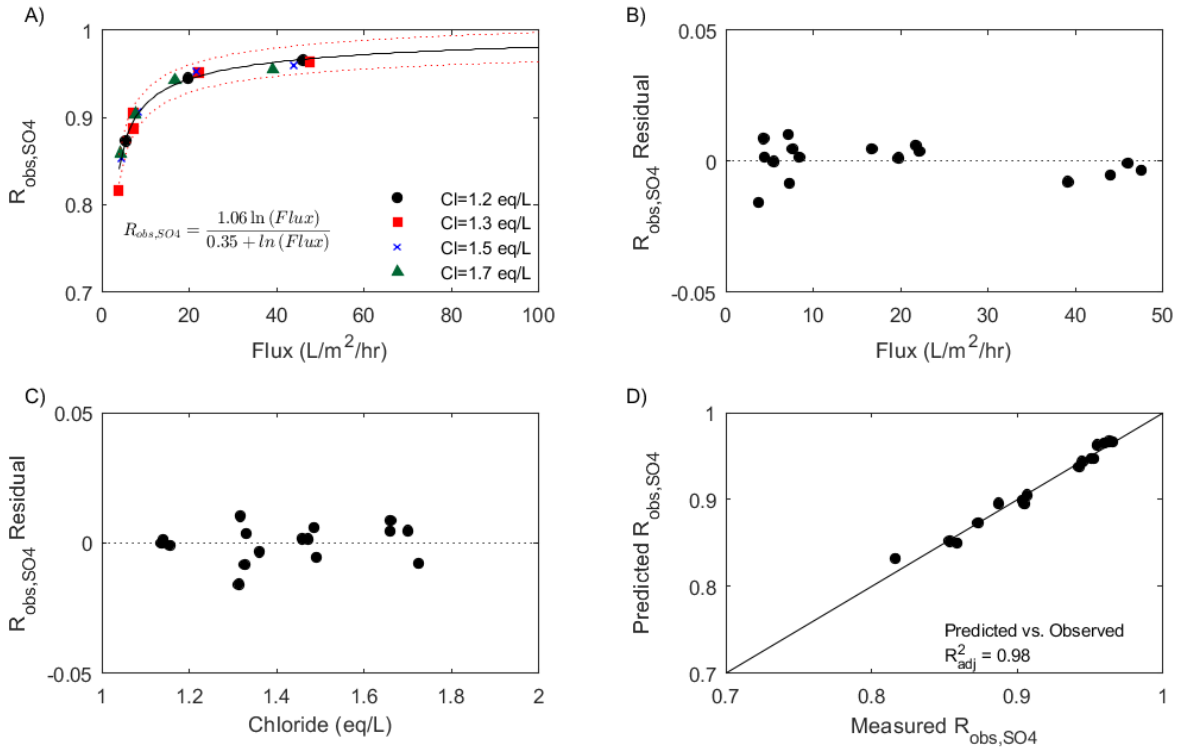

Figure S12. Empirical relationship for predicting sulfate rejection as a function of flux at 250 psi TMP.

In summary, the experiments with synthetic solutions modeling the range of chloride and sulfate concentrations present in SBIX brines yielded response surfaces that can be used to model the cyclical loading, regeneration, and NF-reuse process at 250 psi TMP. In Equation S 26 to Equation S 29, flux has units of L/m^2/hr and all concentrations have units of eq/L.

$$\ln(Flux) = 5 - 1.5[SO_4] - 0.34[Cl] - 0.63[SO_4]^2 \quad \textbf{Equation S 26}$$

$$R_{obs,Cl} = 0.2 - 0.5[SO_4] - 0.07[Cl] + 0.1[SO_4][Cl] + 0.07[SO_4]^2 \quad \textbf{Equation S 27}$$

$$R_{obs,NO3} = -0.2 - 0.2[SO_4] + 0.14[Cl] \quad \textbf{Equation S 28}$$

$$R_{obs,SO4} = \frac{1.1 \ln Flux}{0.35 + \ln Flux} \quad \textbf{Equation S 29}$$

Observed rejections for other trace elements and bicarbonate were defined for the nanofiltration model using experimental data published in Korak et al. (2018). That study measured rejection for three brines from both a full-scale and pilot-scale processes (Figure S13). For each trace metal and bicarbonate, the mean rejection and 95% confidence interval on the mean was calculated and was used in the nanofiltration model. Model outputs will have more uncertainty for vanadium, selenium and bicarbonate compared to other constituents.

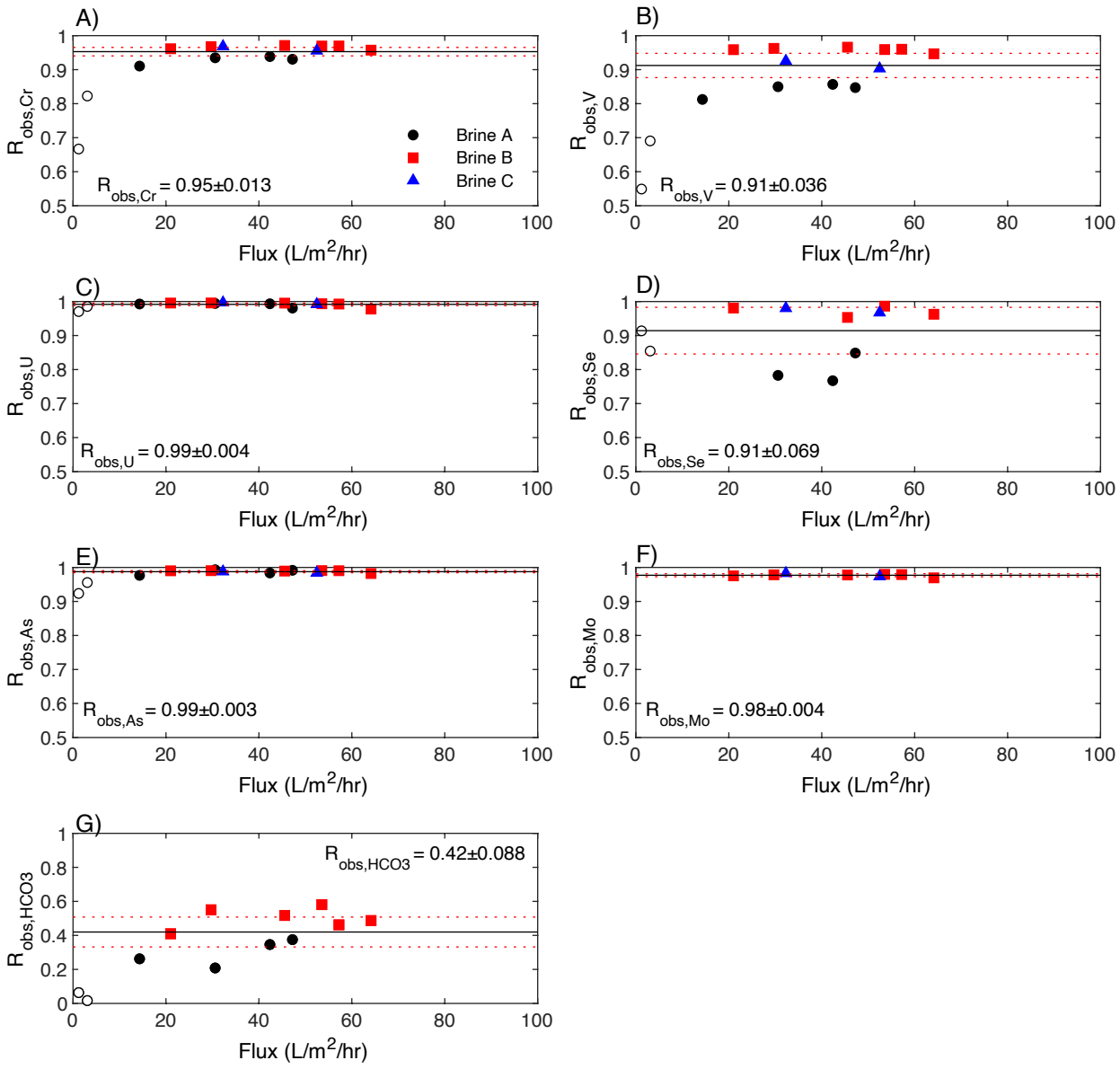

Figure S13. Trace metal rejection as a function of flux from full- and pilot-scale brines at 250 psi TMP. Unfilled markers indicate observations at fluxes less than 5 L/m²/hr. Data was originally published in Korak et al. (2018), but all trace metals were reported in aggregate and not by element.

Assumed average rejections used in the nanofiltration model are shown in Equation S 30 to Equation S 36.

$$R_{obs,Cr} = 0.95 \quad \textbf{Equation S 30}$$

$$R_{obs,V} = 0.91 \quad \textbf{Equation S 31}$$

$$R_{obs,U} = 0.99 \quad \textbf{Equation S 32}$$

$$R_{obs,Se} = 0.91 \quad \textbf{Equation S 33}$$

$$R_{obs,As} = 0.99 \quad \textbf{Equation S 34}$$

$$R_{obs,Mo} = 0.98$$ **Equation S 35**

$$R_{obs,HCO3} = 0.42$$ **Equation S 36**

5.2.3 Impact of TMP on rejection

Additional tests were conducted with the synthetic SBIX brines to investigate the impact of TMP on rejection. The experimental matrix is shown in Table S6 and results are presented in Section 4.1.1 of the main text.

Table S6. Experimental matrix for effect of TMP/flux on rejection.

Batch	$[Cl^-]$ (eq/L)	$[NO_3^-]$ (meq/L)	$[SO_4^{2-}]$ (eq/L)	
1	1.15±0.01	3.0±0.3	0.40±0.01	0.84±0.003
2	1.33±0.02	2.7±0.2	0.37±0.003	0.76±0.002
3	1.49±0.02	2.5±0.2	0.36±0.002	0.74±0.004
4	1.70±0.04	2.7±0.2	0.36±0.003	0.79±0.03
Feed solution pH was adjusted to 8.5 with NaOH and buffered with 1.67 meq/L $NaHCO_3$. Uncertainty represents the standard deviation of feed samples collected in triplicate.				

5.3 Nanofiltration Model

The batch nanofiltration treatment process was discretized into small recovery steps (Rec_j), where *j* represents the recovery increment (e.g., 0.25%, 0.5%, etc.). In each recovery step, waste volume ($V_{w,i,j+1}$) in the Collection Vessel was calculated based on the recovery increment and initial waste volume regeneration cycle ($V_{w,i,0}$) following Equation S 37 and Equation S 38, where *i* represents the regeneration cycle. Note, *i* does not change during the execution of a single nanofiltration batch, but the notation is carried throughout for consistency with the cyclical brine reuse model.

$$\Delta V_{w,i,j+1} = \left(Rec_{j+1} - Rec_j\right)V_{w,i,0}$$ **Equation S 37**

$$V_{w,i,j+1} = V_{w,i,j} - \Delta V_{w,i,j+1}$$ **Equation S 38**

Flux (in units of $L/m^2/hr$) across the membrane during recovery step *j* was calculated according to Equation S 39 based on the chloride ($[Cl]_{w,i,j}$) and sulfate ($[SO4]_{w,i,j}$) concentrations (in [eq/L]) in the Collection Vessel.

$$Flux_j = exp\left(5 - 1.5[SO_4]_{w,i,j} - 0.34[Cl]_{w,i,j} - 0.63{[SO_4]_{w,i,j}}^2\right)$$ **Equation S 39**

The concentration of anions in the permeate ($[C]_{p,i,j+1}$ in eq/L) was determined using the appropriate rejection ($R_{obs,C}$) equation (Equation S 27 to Equation S 36) and the Collection Vessel concentration ($[C]_{w,i,j}$) from the previous recovery step (Equation S 40), where C can be chloride (Cl) or any anion (An) in solution. By mass balance, the new waste concentration ($[C]_{w,i,j+1}$ in eq/L) in the collection vessel was calculated for all anions following Equation S 41.

$$[C]_{p,i,j+1} = \left(1 - R_{obs,C}\right) * [C]_{w,i,j}$$ **Equation S 40**

$$[C]_{w,i,j+1} = \frac{[C]_{w,i,j} * V_{w,i,j} - [C]_{p,i,j+1} * \Delta V_{w,i}}{V_{w,i,j+1}}$$ **Equation S 41**

Sodium concentration in the waste brine ($[Na]_{w,i,j+1}$ in eq/L) and permeate ($[Na]_{P,i,j+1}$ in eq/L) was calculated conforming to electroneutrality as the sum of all anions according to Equation S 42 and Equation S 43.

$$[Na]_{w,i,j+1} = \sum [C]_{w,i,j+1}$$ **Equation S 42**

$$[Na]_{P,i,j+1} = \sum [C]_{P,i,j+1}$$ **Equation S 43**

A composite permeate solution is collected in the NF Permeate Vessel with a volume defined by Equation S 44. Since the composition of the permeate changes as a function of recovery, composite permeate solution concentrations were calculated according to Equation S 45, where C can be any anion. Sodium is calculated based on electroneutrality (Equation S 46).

$$V_{Pcomp,i,j+1} = V_{Pcomp,i,j} + \Delta V_{w,i,j}$$ **Equation S 44**

$$[C]_{Pcomp,i,j+1} = \frac{[C]_{Pcomp,i,j} * V_{Pcomp,i,j} + [C]_{p,i,j+1} * \Delta V_{w,i,j}}{V_{Pcomp,i,j+1}}$$ **Equation S 45**

$$[Na]_{Pcomp,i,j+1} = \sum [C]_{Pcomp,i,j+1}$$ **Equation S 46**

The iterative model was terminated when flux equaled 5 L/m^2/hr, termed the maximum recovery (RecMax). Rejection of divalent anions decreases at low fluxes, which represents a point of diminishing returns for continued waste reduction. At this point, the composition of the waste brine and recycled permeate is defined according to Equation S 47 to Equation S 50

$$V_{Pcomp,i,RecMax} = V_{Pcomp,i,j+1}$$ **Equation S 47**

$$[C]_{Pcomp,i,RecMax} = [C]_{Pcomp,i,j+1}$$ **Equation S 48**

$$V_{w,i,RecMax} = V_{w,i,j+1}$$ **Equation S 49**

$$[C]_{w,i,RecMax} = [C]_{w,i,j+1}$$ **Equation S 50**

6 References

Bissen, M., Frimmel, F.H., 2003. Arsenic — a Review. Part I: Occurrence, Toxicity, Speciation, Mobility. Acta hydrochimica et hydrobiologica 31, 9–18. https://doi.org/10.1002/aheh.200390025

Korak, J.A., Huggins, R., Arias-Paic, M.S., 2018. Nanofiltration to Improve Process Efficiency of Hexavalent Chromium Treatment using Ion Exchange. Journal - American Water Works Association 110, E13–E26. https://doi.org/https://doi.org/10.1002/awwa.1051

Langmuir, D., 1978. Uranium solution-mineral equilibria at low temperatures with applications to sedimentary ore deposits. Geochimica Et Cosmochimica Acta 42, 547–569. https://doi.org/10.1016/0016-7037(78)90001-7

SenGupta, A.K., 1986. Anomalous Ion-Exchange Characteristics of some Poly-Nuclear Metal Ions. Journal of Chromatography 368, 319–328. https://doi.org/10.1016/s0021-9673(00)91074-4

SenGupta, A.K., Clifford, D.A., 1986. Important Process Variables in Chromate Ion Exchange. Environmental Science & Technology 20, 155–160.

White, A.F., Dubrovsky, N.M., 1994. Chemical Oxidation-Reduction Controls on Selenium Mobility in Groundwater Systems, in: Selenium in the Environment. CRC Press, pp. 185–222.

Wright, M.T., Stollenwerk, K.G., Belitz, K., 2014. Assessing the solubility controls on vanadium in groundwater, northeastern San Joaquin Valley, CA. Applied Geochemistry 48, 41–52. https://doi.org/10.1016/j.apgeochem.2014.06.025

Zhang, Z., Clifford, D.A., 1994. Exhausting and regenerating resin for uranium removal 86, 228–241. https://doi.org/10.1002/j.1551-8833.1994.tb06184.x